Quantum logic with weakly coupled qubits

Michael R. Geller,[1] Emily J. Pritchett,[1] Andrei Galiautdinov,[1] and John M. Martinis[2]

[1]*Department of Physics and Astronomy, University of Georgia, Athens, Georgia 30602, USA*

[2]*Department of Physics, University of California, Santa Barbara, California 93106, USA*

There are well-known protocols for performing controlled NOT (CNOT) quantum logic with qubits coupled by particular high-symmetry (Ising or Heisenberg) interactions. However, many architectures being considered for quantum computation involve qubits or qubits and resonators coupled by more complicated and less symmetric interactions. Here we consider a widely applicable model of weakly but otherwise arbitrarily coupled two-level systems, and use quantum gate design techniques to derive a simple and intuitive CNOT construction. Useful variations and extensions of the solution are given for common special cases.

I. QUANTUM GATE DESIGN

Experimental realizations of gate-based quantum computation require the accurate implementation of universal two-qubit operations such as the controlled-NOT (CNOT) quantum logic gate [1]. Finding the best way to achieve this for a specific experimental architecture is a principal goal of what we refer to as *quantum gate design*. The CNOT problem can be informally stated as follows: Specify the dimension N of the relevant Hilbert space, and a Hamiltonian

$$H(\xi_1, \xi_2, \ldots, \xi_K) \tag{1}$$

with some experimental control over K parameters $\xi_1, \ldots, \xi_K$. How should the control parameters be varied to generate CNOT logic in the computational basis $\{|00\rangle, |01\rangle, |10\rangle, |11\rangle\}$? For a closed system this is a control problem in the unitary group $U(N)$. N is not necessarily equal to 4 because the Hamiltonian might include auxiliary non-qubit states (not in the computational basis) that help implement the logic. For example, an effective strategy (see, for example, Strauch *et al.* [2] and DiCarlo *et al.* [3]) is to use an anticrossing of the $|11\rangle$ state with a noncomputational state $|\text{aux}\rangle$ to generate a 2π rotation in the two-dimensional subspace $\{|11\rangle, |\text{aux}\rangle\}$. This implements the gate

$$\text{CZ} \equiv \begin{pmatrix} 1 & 0 & 0 & 0 \\ 0 & 1 & 0 & 0 \\ 0 & 0 & 1 & 0 \\ 0 & 0 & 0 & -1 \end{pmatrix} \tag{2}$$

in the computational basis, out of which a CNOT gate can be constructed by pre- and postapplication of single-qubit Hadamard gates (see below). Another important example is Cirac and Zoller's use of vibrational modes to mediate quantum logic between the internal qubit states of trapped ions [4,5].

In the familiar $U(4)$ case, the Hamiltonian (1) can be written in terms of Pauli matrices and their tensor products. The resulting coupled-qubit model usually allows control of some of the single-qubit operators—enough to perform arbitrary $SU(2)$ rotations on each qubit—and possibly of the qubit-qubit coupling. For certain commonly occurring forms of the qubit-qubit interaction, including the highly symmetric cases of Ising-like $\sigma_1^z \sigma_2^z$ interaction [1] and Heisenberg-like $\boldsymbol{\sigma}_1 \cdot \boldsymbol{\sigma}_2$ interaction [6], effective protocols for implementing CNOT

gates have been established. However, many architectures being considered for quantum computation involve qubits or qubits and resonators coupled by more complicated and less symmetric interactions, or would be more accurately modeled as such.

Here we investigate the general problem of weakly but otherwise arbitrarily coupled qubits, and use perturbation theory combined with other quantum gate design techniques to derive a simple and widely applicable CNOT pulse construction. Useful variations and extensions of the basic solution are given for common special cases, and the intuitive geometric picture we employ—related to the Weyl chamber description introduced by Zhang *et al.* [7]—will be useful elsewhere in the design of quantum logic gates. We assume unitary evolution, which is sensible given the generality of our result and the wide variation in experimental coherence times.

Zhang *et al.* [7] and Zhang and Whaley [8] have addressed the problem of two-qubit gate construction using similar methods applied to a variety of coupled-qubit models, but focused on steering with continuous rf control as opposed to the short pulses considered below. One of us has recently investigated the implementation of CNOT gates using constant rf driving [9,10] and also moderately detuned qubits [11], providing constructions complementary to those presented here. Time-optimal and other direct quantum control approaches are especially useful for strongly coupled and/or strongly driven qubits, or to optimize performance in the presence of specific decohering and/or noisy environments [12–18], but early quantum logic demonstrations might best be accomplished using the simple perturbative protocol described here.

II. WEAKLY COUPLED QUBITS

In a wide variety of physical systems being considered for quantum computation, the Hamiltonian for a pair of coupled qubits can be written (suppressing $\hbar$) as

$$H = \sum_{i=1,2} \left[-\frac{\epsilon_i}{2} \sigma_i^z + \Omega_i \cos(\epsilon_i t + \phi_i) \sigma_i^x \right]$$
$$+ \sum_{\mu,\nu=x,y,z} J_{\mu\nu} \sigma_1^\mu \otimes \sigma_2^\nu, \tag{3}$$

with $J_{\mu\nu}$ a 3×3 real-valued tensor (possibly adjustable). The Hamiltonian (3) is written in the basis of eigenstates ($|0\rangle$ and

$|1\rangle$) of uncoupled qubits with energy level spacings ϵ_i, and the parameters ϵ_i and Ω_i (with $\Omega_i \ll \epsilon_i$) are assumed to be experimentally controllable. More general single-qubit control is often available but will not be needed here. Our principal assumption is that of weak coupling: The magnitude of the $J_{\mu\nu}$ are assumed to be small compared with the ϵ_i.

Two-qubit logic gates will be implemented by combining certain entangling operations, performed with tuned ($\epsilon_1 = \epsilon_2$) qubits, together with single-qubit operations performed with detuned or decoupled qubits [19]. In a frame rotating with the frequency of the tuned qubits, the Hamiltonian (3) reduces approximately to [20]

$$H \approx \sum_{i=1,2} \frac{\Omega_i}{2}\big(\cos\phi_i \, \sigma_i^x - \sin\phi_i \, \sigma_i^y\big) + \mathcal{H}, \qquad (4)$$

where

$$\mathcal{H} \equiv J\big(\sigma_1^x\sigma_2^x + \sigma_1^y\sigma_2^y\big) + J_{zz}\,\sigma_1^z\sigma_2^z + J'\big(\sigma_1^x\sigma_2^y - \sigma_1^y\sigma_2^x\big). \qquad (5)$$

Here

$$J \equiv \frac{J_{xx} + J_{yy}}{2} \quad \text{and} \quad J' \equiv \frac{J_{xy} - J_{yx}}{2} \qquad (6)$$

are real coupling constants. In the computational basis,

$$\mathcal{H} = \begin{pmatrix} J_{zz} & 0 & 0 & 0 \\ 0 & -J_{zz} & \gamma & 0 \\ 0 & \gamma^* & -J_{zz} & 0 \\ 0 & 0 & 0 & J_{zz} \end{pmatrix}, \qquad (7)$$

where

$$\gamma \equiv 2(J + iJ') = |\gamma|\,e^{i\varphi}. \qquad (8)$$

To obtain Eq. (4) we have assumed that the $J_{\mu\nu}$ and Ω_i are small compared with the qubit frequency and have neglected the resulting rapidly oscillating terms with vanishing time-averages; this is the usual rotating-wave approximation (RWA). Although nine coupling constants are present in Eq. (3), only three parameters appear in $\mathcal{H}$, making a general analysis possible. The terms in Eq. (5) multiplying J and J_{zz} are symmetric under qubit-label exchange, whereas the J' term is antisymmetric and therefore vanishes when the physical qubits in question (and their operating biases) are identical. Furthermore, in the common case of $J' = 0$ (which must occur when the qubits are identical but can also occur when they are not), $\mathcal{H}$ commutes with itself at different times when J and J_{zz} are time dependent, leading to additional flexibility (in the form of "area" theorems) for pulse design that we will use below. We emphasize that $\mathcal{H}$ is a universal Hamiltonian, applying to any pair of tuned, weakly coupled qubits. Coupled-qubit models with nondiagonal single-qubit terms can be put in the form (3) after transformation to the uncoupled eigenstate basis.

The CNOT pulse sequence derived below is valid whenever

$$J^2 + J'^2 \neq 0. \qquad (9)$$

The condition (9) excludes qubit-qubit interactions of the Ising form

$$\delta H = g\,\sigma_1^z\sigma_2^z, \qquad (10)$$

for which an effective single-entangling-pulse construction is already known, as well as interactions such as

$$\delta H = g\big(\sigma_1^x\sigma_2^x - \sigma_1^y\sigma_2^y\big), \qquad (11)$$

that *vanish* in the RWA.

III. CARTAN DECOMPOSITION

The trajectory in U(4) that the evolution operator

$$U \equiv T\,e^{-i\int_0^t H\,d\tau} \qquad (12)$$

traces out during Schrödinger evolution (T is the time-ordering operator) can be viewed by factoring out local (single-qubit) rotations

$$u \in \mathrm{SU}(2) \otimes \mathrm{SU}(2). \qquad (13)$$

A convenient way to achieve this is to use the fact that any element of U(4) can be written as

$$U = e^{i\phi}\,u_{\mathrm{post}}\,A\,u_{\mathrm{pre}}, \qquad (14)$$

with

$$A(x, y, z) \equiv e^{-i(x\,\sigma_1^x\sigma_2^x + y\,\sigma_1^y\sigma_2^y + z\,\sigma_1^z\sigma_2^z)}, \qquad (15)$$

for some local rotations u_{pre} and u_{post}, real-valued coordinates (angles) x, y, and z, and global phase ϕ. This formula can be derived by using a Cartan decomposition of the Lie algebra $su(4)$ [12,21–23]. The central component A, which we call the *entangler*, characterizes the nonlocal or entangling part of U and is a periodic function of its coordinates with period 2π. By performing the decomposition (14) at each time t and forming the vector $\vec{r} \equiv (x, y, z)$, we can view the evolution of the nonlocal part of U as a trajectory $\vec{r}(t)$ through the three-dimensional toroidal space of entanglers [7]. A special property of Eq. (15) is that the generators $\sigma^x \otimes \sigma^x$, $\sigma^y \otimes \sigma^y$, and $\sigma^z \otimes \sigma^z$ all commute (they form a Cartan subalgebra). The minus sign introduced into the exponent of Eq. (15) simplifies the analysis in the common special case of $J' = 0$.

The decomposition (14) into an entangler A, local rotations u_{pre} and u_{post}, and phase factor $e^{i\phi}$ is not unique. This means that the trajectory $\vec{r}(t)$ corresponding to some actual physical evolution is not unique. But the different options for A at each time t are evidently *locally equivalent* (differing by pre- and postapplication of local rotations and a multiplicative phase factor). Furthermore, in the common special case of $J' = 0$, a particularly natural continuous solution [given in Eq. (19) below] can always be chosen which has the simplifying property that the local rotations and phase factor are equal to the identity along the entire trajectory: The local rotation and global phase angles vanish. We note that the usefulness of the decomposition (14) goes far beyond its somewhat technical role here: (i) In architectures where local operations can be performed quickly and accurately (they are "free"), the decomposition allows one to focus directly on the remaining nonlocal part; (ii) The local rotations associated with successive gates can often be combined; And (iii), some of the experimental error incurred when implementing an entangler—the component that does not change the equivalence class—can be corrected by modifying the u's.

The concepts of local equivalence and local equivalence classes have wide application in gate design. Makhlin [24] has constructed an explicit formula for three quantities that can be used to test for local equivalence. The CNOT gate [25]

$$\text{CNOT} \equiv \begin{pmatrix} 1 & 0 & 0 & 0 \\ 0 & 1 & 0 & 0 \\ 0 & 0 & 0 & 1 \\ 0 & 0 & 1 & 0 \end{pmatrix} \tag{16}$$

has Makhlin invariants $G_1 = 0$ and $G_2 = 1$ (G_1 is generally complex). Two members U and U' of U(4) are locally equivalent if and only if their Makhlin invariants are identical, in which case we write $U \sim U'$. When restricted to a certain (nearly) tetrahedral region—a Weyl chamber—the angles x, y, and z are in one-to-one correspondence with the Makhlin invariants, leading to a unique $\vec{r}$ and a useful geometric description of the local equivalence classes of U(4) [7]. For our purposes, however, it will be convenient to work in the full toroidal space of entanglers and not restrict $\vec{r}$ to a Weyl chamber [26].

IV. CNOT CONSTRUCTION FOR THE CASE OF $J' = 0$

First we consider the common special case of Hamiltonian (5) with $J' = 0$, which includes the case of identical qubits. Assuming tuned qubits and no rf drive, the evolution (12) dramatically simplifies to

$$U = A(x, y, z) \tag{17}$$

with entangler coordinates

$$x = y = \int_0^t J \, d\tau,$$
$$z = \int_0^t J_{zz} \, d\tau. \tag{18}$$

This evolution follows a curve in the vertical plane $x = y$. The trajectory for the case of time-independent J and J_{zz} is illustrated in Fig. 1. The fact that the coordinates (19) of the generated entangler depend only on time-integrals of the coupling constants indicates a type of robustness and flexibility of the associated experimental pulse sequence, analogous to the area theorem for single-qubit rotations within the RWA. The closest CNOT-class entanglers are at $\vec{r} = (\pm\frac{\pi}{4}, 0, 0)$, $(0, \pm\frac{\pi}{4}, 0)$, and $(0, 0, \pm\frac{\pi}{4})$, which cannot be reached with one application of $\mathcal{H}$ unless J vanishes. In this Ising case, $A(0, 0, \frac{\pi}{4})$ or $A(0, 0, -\frac{\pi}{4})$ is obtained after

$$\int J_{zz} \, d\tau = \pm\frac{\pi}{4} \pmod{2\pi}. \tag{19}$$

Generating one of these entanglers corresponds to generating a particular member of the CNOT equivalence class; either one is sufficient. A possible Ising pulse sequence (executed from right to left) is [27]

$$\text{CNOT} = e^{\mp i\frac{\pi}{4}} \, \mathsf{H}_2 \, R_z\left(\mp\frac{\pi}{2}\right)_1 \, R_z\left(\mp\frac{\pi}{2}\right)_2 \, A\left(0, 0, \pm\frac{\pi}{4}\right) \mathsf{H}_2, \tag{20}$$
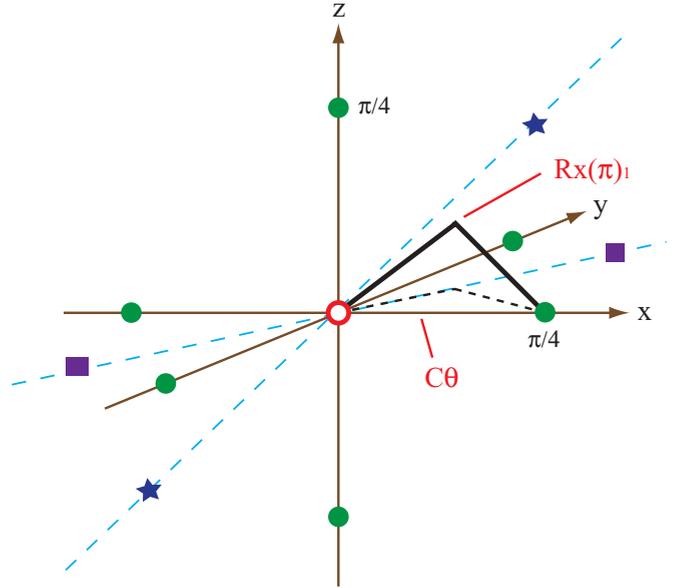
FIG. 1. (Color online) Three-dimensional space of entanglers A, showing the six members $A(\pm\frac{\pi}{4}, 0, 0)$, $A(0, \pm\frac{\pi}{4}, 0)$, and $A(0, 0, \pm\frac{\pi}{4})$ of the CNOT equivalence class (solid/green circles) closest to the identity (open/red circle). The Schrödinger evolution resulting from Eq. (5) with *fixed* positive J and J_{zz} is indicated by the black trajectory, interrupted by the application of a fast π pulse. The (purple) square at $\vec{r} = (\frac{\pi}{4}, \frac{\pi}{4}, 0)$ is locally equivalent to the CNOT $\times$ SWAP and SWAP $\times$ CNOT gates, and the blue star at $\vec{r} = (\frac{\pi}{4}, \frac{\pi}{4}, \frac{\pi}{4})$ is locally equivalent to the SWAP.

where

$$\mathsf{H} \equiv i \, R_x(\pi) \, R_y\left(\frac{\pi}{2}\right) \tag{21}$$

is a Hadamard gate.

Another important special case occurs when J_{zz} vanishes, often called an *XY* interaction [28]. Here one can follow the general two-entangling-pulse protocol detailed below to generate the canonical CNOT gate (16) or, alternatively, one can generate the entangler $A(\frac{\pi}{4}, \frac{\pi}{4}, 0)$ or $A(-\frac{\pi}{4}, -\frac{\pi}{4}, 0)$ in a single shot. These entanglers are locally equivalent to both

$$\text{CNOT} \times \text{SWAP}$$

and

$$\text{SWAP} \times \text{CNOT},$$

where

$$\text{SWAP} \equiv \begin{pmatrix} 1 & 0 & 0 & 0 \\ 0 & 0 & 1 & 0 \\ 0 & 1 & 0 & 0 \\ 0 & 0 & 0 & 1 \end{pmatrix} \tag{22}$$

is the SWAP gate. The gates CNOT $\times$ SWAP and SWAP $\times$ CNOT are as effective as Eq. (16) in the sense that any quantum circuit written in terms of CNOT gates can be immediately rewritten in terms of the swapped versions with no overhead. These gates are also equivalent to double-CNOT gates, consisting of a pair targeting each qubit in succession

(see remark [25]):

$$\text{SWAP} \times \text{CNOT} = \text{CNOT} \times \left(\text{SWAP}\,\text{CNOT}\,\text{SWAP}\right)$$

$$\text{CNOT} \times \text{SWAP} = \left(\text{SWAP}\,\text{CNOT}\,\text{SWAP}\right) \times \text{CNOT}.$$

The effectiveness of the double-CNOT gate is discussed in Ref. [29], where quantum circuits implementing arbitrary two-qubit unitary transformations with three CNOT gates or three double-CNOT gates (the minimum numbers possible) are given. Pulse sequences for constructing a SWAP × CNOT gate from the entangler $A(\frac{\pi}{4}, \frac{\pi}{4}, 0)$ or $A(-\frac{\pi}{4}, -\frac{\pi}{4}, 0)$ are

$$\begin{aligned}
\text{SWAP} \times \text{CNOT} = &\pm i \left[R_x \left(\pm\frac{\pi}{2}\right)_1 \, R_x \left(\frac{\pi}{2}\right)_2 \right] \\
&\times \left[R_y \left(\frac{\pi}{2}\right)_1 R_y \left(\pm\frac{\pi}{2}\right)_2 \right] R_x \left(-\frac{\pi}{2}\right)_2 \\
&\times A \left(\pm\frac{\pi}{4}, \pm\frac{\pi}{4}, 0\right) R_y \left(-\frac{\pi}{2}\right)_2.
\end{aligned} \quad (23)$$

Operations grouped together in square brackets can be performed simultaneously.

Although CNOT-class entanglers farther from the origin (and not shown in Fig. 1) can be reached in one shot for special values of J_{zz}/J, a faster and more generally applicable protocol is to interrupt the evolution with a fast refocusing π pulse applied to either qubit. A pair of such pulses enclosing an interval of tuned qubit evolution

$$\cdots R_x(-\pi)\, e^{-i\int \mathcal{H}\,d\tau}\, R_x(\pi) \cdots \quad (24)$$

can be viewed as transforming the interaction Hamiltonian during that interval to (note sign changes)

$$R_x^\dagger(\pi)\,\mathcal{H}\,R_x(\pi) = J\left(\sigma_1^x \sigma_2^x - \sigma_1^y \sigma_2^y\right) - J_{zz}\,\sigma_1^z \sigma_2^z, \quad (25)$$

causing the reflection illustrated in Fig. 1 and allowing the evolution to reach any entangler on the positive x axis (or negative axis for $J < 0$). Similarly, $R_y(\pi)$ rotations would cause a reflection toward the y axis. In what follows we will apply refocusing pulses to the first qubit.

By a direct calculation of Makhlin invariants it can be shown that entanglers on the x, y and z axes are locally equivalent to each other and to the controlled-phase gate

$$\mathrm{C}\theta \equiv \begin{pmatrix} 1 & 0 & 0 & 0 \\ 0 & 1 & 0 & 0 \\ 0 & 0 & 1 & 0 \\ 0 & 0 & 0 & e^{i\theta} \end{pmatrix} \sim A\left(\frac{\theta}{4}, 0, 0\right) \sim A\left(0, \frac{\theta}{4}, 0\right)$$

$$\sim A\left(0, 0, \frac{\theta}{4}\right). \quad (26)$$

The entanglers at $\vec{r} = (\pm\frac{\pi}{4}, 0, 0)$, shown in Fig. 1 as solid/green circles, are thus locally equivalent to the CZ gate (2), and hence to the CNOT gate. The identity

$$R_x(-\pi)_1 \, A\left(\pm\frac{\pi}{8}, \pm\frac{\pi}{8}, z\right) R_x(\pi)_1 = A\left(\pm\frac{\pi}{8}, \mp\frac{\pi}{8}, -z\right),$$

with z arbitrary, allows us to reach

$$A\left(\pm\frac{\pi}{8}, \mp\frac{\pi}{8}, -z\right) A\left(\pm\frac{\pi}{8}, \pm\frac{\pi}{8}, z\right) = A\left(\pm\frac{\pi}{4}, 0, 0\right) \quad (27)$$

after two entangling intervals, out of which a CNOT gate can be constructed according to

$$\begin{aligned}
\text{CNOT} = &e^{\mp i\frac{\pi}{4}} R_y \left(-\frac{\pi}{2}\right)_1 \left[R_x \left(\mp\frac{\pi}{2}\right)_1 R_x \left(\mp\frac{\pi}{2}\right)_2 \right] \\
&\times A\left(\pm\frac{\pi}{4}, 0, 0\right) R_y \left(\frac{\pi}{2}\right)_1.
\end{aligned} \quad (28)$$

More explicitly, we can write this pulse sequence as

$$\begin{aligned}
\text{CNOT} = &e^{\mp i\frac{\pi}{4}} R_y \left(-\frac{\pi}{2}\right)_1 \left[R_x \left(\mp\frac{\pi}{2}\right)_1 R_x \left(\mp\frac{\pi}{2}\right)_2 \right] \\
&\times R_x(-\pi)_1 A\left(\pm\frac{\pi}{8}, \pm\frac{\pi}{8}, z\right) R_x(\pi)_1 \\
&\times A\left(\pm\frac{\pi}{8}, \pm\frac{\pi}{8}, z\right) R_y \left(\frac{\pi}{2}\right)_1,
\end{aligned} \quad (29)$$

where either $A\left(\frac{\pi}{8}, \frac{\pi}{8}, z\right)$ or $A\left(-\frac{\pi}{8}, -\frac{\pi}{8}, z\right)$ is produced by the application of $\mathcal{H}$ for a time such that $\int J\,d\tau = \frac{\pi}{8}$ or $-\frac{\pi}{8}$, depending on the sign of J.

V. ARBITRARY J'

Here we assume the Hamiltonian (5) with fixed, time-independent values of J, J_{zz}, and J' (excluding the case $J^2 + J'^2 = 0$). When $J' \neq 0$ there are terms in the Hamiltonian that are not in the Cartan subalgebra and that break the symmetry under qubit exchange. Such terms can be eliminated by performing a z rotation on the second qubit by an angle $\varphi \equiv \arg(J + iJ')$,

$$\begin{aligned}
R_z^\dagger(\varphi)_2\,\mathcal{H}\,R_z(\varphi)_2 = &\sqrt{J^2 + J'^2}\left(\sigma_1^x \sigma_2^x + \sigma_1^y \sigma_2^y\right) \\
&+ J_{zz}\,\sigma_1^z \sigma_2^z,
\end{aligned} \quad (30)$$

allowing us to reach the CNOT-class entangler

$$\begin{aligned}
A\left(\frac{\pi}{4}, 0, 0\right) = &R_z(-\varphi)_2 R_x(-\pi)_1 \, e^{-i\mathcal{H}\,\Delta t} \\
&\times R_x(\pi)_1 \, e^{-i\mathcal{H}\,\Delta t} R_z(\varphi)_2.
\end{aligned} \quad (31)$$

Here $e^{-i\mathcal{H}\,\Delta t}$ represents the action of bringing the qubits into resonance for a time

$$\Delta t \equiv \frac{\pi}{8\sqrt{J^2 + J'^2}}. \quad (32)$$

The complete pulse sequence in this case can be written as

$$\begin{aligned}
\text{CNOT} = &e^{i\left(\frac{3\pi}{4}\right)} \left[R_y \left(-\frac{\pi}{2}\right)_1 R_x \left(-\frac{\pi}{2}\right)_2 \right] R_z(-\varphi)_2 \\
&\times R_x \left(\frac{\pi}{2}\right)_1 e^{-i\mathcal{H}\,\Delta t} R_x(\pi)_1 e^{-i\mathcal{H}\,\Delta t} R_z(\varphi)_2 R_y \left(\frac{\pi}{2}\right)_1.
\end{aligned} \quad (33)$$

VI. DISCUSSION

In conclusion, we have investigated the CNOT gate design problem for a widely applicable four-dimensional model of weakly but otherwise arbitrarily coupled qubits. The qubit-qubit interaction Hamiltonian in the RWA can always be written in the form (5), which contains only three real coupling constants. In the common case of physically identical (and identically biased) qubits, J' vanishes, and the most general interaction is that of the anisotropic Heisenberg model. In this case the time evolution operator is simply given by Eq. (17), with entangler coordinates (19). Refocusing π pulses applied to the first qubit reflect that entangler trajectory to the x axis,

leading to the CNOT pulse sequence (29). We note that when $J' = 0$ the entangling pulses can be generated with either time-independent or time-dependent interaction parameters J and J_{zz}. The case when $J' \neq 0$ follows similarly after an additional single-qubit rotation $R_z(\varphi)_2$, leading to the pulse sequence (33). Here, however, the entanglers are generated with fixed interaction parameters by bringing the qubits into resonance for a time (32).

[1] M. A. Neilsen and I. L. Chuang, *Quantum Computation and Quantum Information* (Cambridge University Press, Cambridge, UK, 2000).

[2] F. W. Strauch, P. R. Johnson, A. J. Dragt, C. J. Lobb, J. R. Anderson, and F. C. Wellstood, Phys. Rev. Lett. **91**, 167005 (2003).

[3] L. DiCarlo, J. M. Chow, J. M. Gambetta, L. S. Bishop, D. I. Schuster, J. Majer, A. Blais, L. Frunzio, S. M. Girvin, and R. J. Schoelkopf, Nature (London) **460**, 240 (2009).

[4] J. I. Cirac and P. Zoller, Phys. Rev. Lett. **74**, 4091 (1995).

[5] C. Monroe, D. M. Meekhof, B. E. King, W. M. Itano, and D. J. Wineland, Phys. Rev. Lett. **75**, 4714 (1995).

[6] D. Loss and D. P. DiVincenzo, Phys. Rev. A **57**, 120 (1998).

[7] J. Zhang, J. Vala, S. Sastry, and K. B. Whaley, Phys. Rev. A **67**, 042313 (2003).

[8] J. Zhang and K. B. Whaley, Phys. Rev. A **71**, 052317 (2005).

[9] A. Galiautdinov, Phys. Rev. A **75**, 052303 (2007).

[10] A. Galiautdinov, J. Math. Phys. **48**, 112105 (2007).

[11] A. Galiautdinov, Phys. Rev. A **79**, 042316 (2009).

[12] N. Khaneja, R. Brockett, and S. J. Glaser, Phys. Rev. A **63**, 032308 (2001).

[13] P. Zanardi and S. Lloyd, Phys. Rev. A **69**, 022313 (2004).

[14] I. A. Grigorenko and D. V. Khveshchenko, Phys. Rev. Lett. **94**, 040506 (2005).

[15] I. A. Grigorenko and D. V. Khveshchenko, Phys. Rev. Lett. **95**, 110501 (2005).

[16] A. Spörl, T. Schulte-Herbrüggen, S. J. Glaser, V. Bergholm, M. J. Storcz, J. Ferber, and F. K. Wilhelm, Phys. Rev. A **75**, 012302 (2007).

[17] P. Rebentrost, I. Serban, T. Schulte-Herbrüggen, and F. K. Wilhelm, Phys. Rev. Lett. **102**, 090401 (2009).

[18] F. Motzoi, J. M. Gambetta, P. Rebentrost, and F. K. Wilhelm, Phys. Rev. Lett. **103**, 110501 (2009).

[19] When $J_{zz} \neq 0$, the interaction between detuned qubits is *not* suppressed, and it is preferable to switch off the coupling during single-qubit operations in this case.

[20] Transformation to a frame rotating with qubit frequencies ϵ_1 and ϵ_2 is defined according to $|\psi\rangle \rightarrow \chi|\psi\rangle$, where $\chi \equiv \prod_i R_z(\int \epsilon_i dt)_i$. Under this transformation, $\sigma_i^\mu \rightarrow \chi \sigma_i^\mu \chi^\dagger = \sum_\nu \mathcal{R}_z^{\mu\nu}(\int \epsilon_i dt)\sigma_i^\nu$, where

$$\mathcal{R}_z(\alpha) \equiv \begin{pmatrix} \cos\alpha & \sin\alpha & 0 \\ -\sin\alpha & \cos\alpha & 0 \\ 0 & 0 & 1 \end{pmatrix}$$

is an SO(3) rotation matrix.

[21] N. Khaneja and S. J. Glaser, Chem. Phys. **267**, 11 (2001).

[22] B. Kraus and J. I. Cirac, Phys. Rev. A **63**, 062309 (2001).

[23] S. Helgason, *Differential Geometry, Lie Groups, and Symmetric Spaces* (American Mathematical Society, Providence, 1978).

[24] Y. Makhlin, Quant. Info. Proc. **1**, 243 (2002).

[25] The CNOT operator defined in Eq. (16) specifies qubit 1 to be the control qubit. The locally equivalent alternative controlling the second qubit is SWAP × CNOT × SWAP.

[26] We also adopt a slightly different notation than that of Ref. [7], writing $\vec{c}$ as $-2\vec{r}$.

[27] $R_\mu(\theta)_i \equiv e^{-i(\theta/2)\sigma_i^\mu}$ is a μ rotation on qubit i.

[28] Pulse sequences for the XY case were previously derived in unpublished notes by Matthias Steffen.

[29] J. Zhang, J. Vala, S. Sastry, and K. B. Whaley, Phys. Rev. A **69**, 042309 (2004).